CONCEPTS

Gene Delivery

C. Ortiz Mellet, J. M. Benito, J. M. García Fernández** . . . 6728 – 6742

Preorganized, Macromolecular, Gene-Delivery Systems

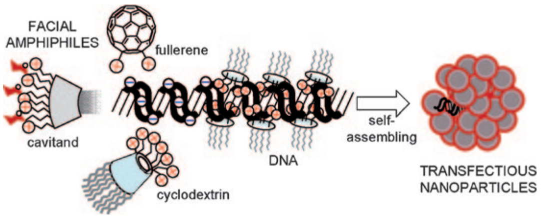

Artificial viruses from monodisperse compounds: Preorganization of functional elements onto macromolecular platforms has the potential to allow control of the self-assembling behavior of discrete architectures to produce nanometric objects that can be programmed to complex, compact, deliver, and release plasmid DNA in a target cell (see graphic).

COMMUNICATIONS

Supramolecular Chemistry

*M. Altman, M. Rachamim, T. Ichiki, M. A. Iron, G. Evmenenko, P. Dutta, M. E. van der Boom** . . . . 6744 – 6747

Designing Surface-Confined Coordination Oligomers

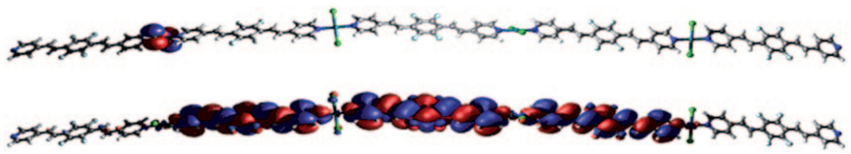

Designer materials: HOMO–LUMO engineering of coordination-based oligomers covalently bound to silicon or glass has been achieved by the use of a partially fluorinated chromophore (see graphic). The experimental and computationally derived physical chemical properties of these assemblies are compared to their non-fluorinated analogues.

Biphasic Catalysis

*V. Gauchot, W. Kroutil, A. R. Schmitzer** . . . . 6748 – 6751

Highly Recyclable Chemo-/Biocatalyzed Cascade Reactions with Ionic Liquids: One-Pot Synthesis of Chiral Biaryl Alcohols

Mix and match: We report a cascade reaction sequence for the highly enantio- and diastereoselective synthesis of biaryl alcohols, employing a Suzuki coupling followed by a biocatalytic reduction in a biphasic system containing ionic liquids (ILs; see figure). We demonstrate the recyclability of the IL phase as well as the aqueous phase up to four cycles with only a negligible deactivation of reactivity and selectivity.

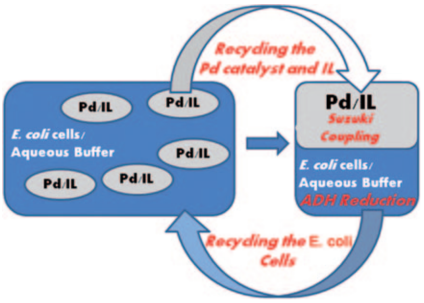

Asymmetric Catalysis

*N. Ototake, Y. Morimoto, A. Mokuya, H. Fukaya, Y. Shida, O. Kitagawa** . . . . 6752 – 6755

Catalytic Enantioselective Synthesis of Atropisomeric Indoles with an N–C Chiral Axis

A pivotal role: In the presence of (*R*)-(−)-5,5′-bis[di(3,5-di-*tert*-butyl-4-methoxyphenyl)phosphino]-4,4′-bi-1,3-benzodioxole–$PdCl_2$ [(*R*)-SEGPHOS–$PdCl_2$], 5-*endo*-hydroaminocyclization of achiral *ortho*-alkynylanilines proceeds in an enantioselective manner to give optically active, axially chiral indoles (see scheme).

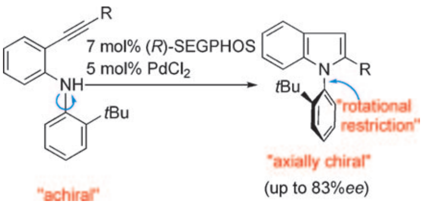

Stilbenes

J. McNulty, P. Das, D. McLeod* .... 6756 – 6760

Microwave-Assisted, Aqueous Wittig Reactions: Organic-Solvent- and Protecting-Group-Free Chemoselective Synthesis of Functionalized Alkenes

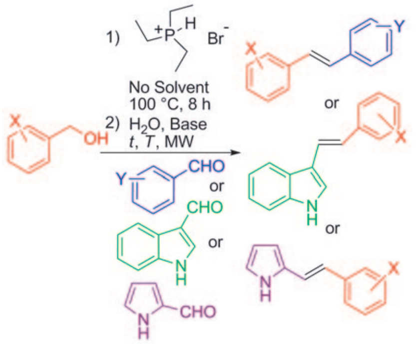

Free from protection! A general, chemoselective, protecting-group- and organic-solvent-free route to stilbenes and heterostilbenes involving the direct synthesis of triethyl benzylic and allylic phosphonium salts from the corresponding alcohols and their microwave-assisted, aqueous Wittig reactions is described.

Asymmetric Catalysis

L. Cheng, J. Dong, J. You, G. Gao, J. Lan** .... 6761 – 6765

A Highly *syn*-Selective Nitroaldol Reaction Catalyzed by Cu^{II}–Bisimidazoline

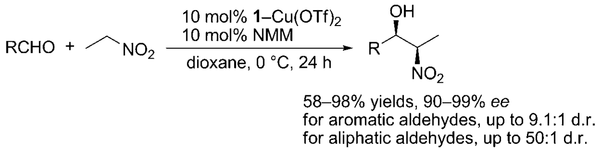

Catalyzing Henry: Chiral bisimidazoline **1**–$Cu(OTf)_2$, in the presence of *N*-methylmorpholine as a base, was discovered to efficiently catalyze the nitroaldol reaction in a highly *syn*- and enantioselective manner for a broad range of aldehydes, including aromatic, heteroaromatic, α,β-unsaturated, and aliphatic aldehydes (see scheme).

Electrode Potentials

Y.-M. Fang, Z.-B. Lin, Y.-M. Zeng, W.-K. Chen, G.-N. Chen, J.-J. Sun, B. Ren,* Z.-Q. Tian* .... 6766 – 6770

Facile Electrochemical Preparation of Ag Nanothorns and Their Growth Mechanism

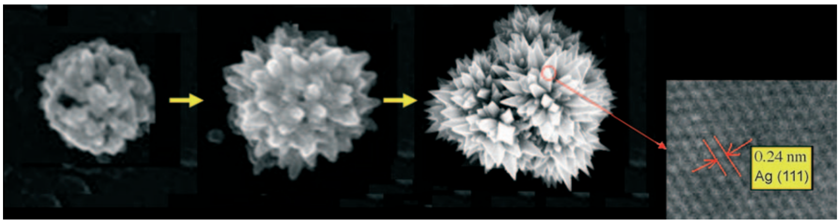

Prickly silver: Ag nanothorn assemblies with large-scale (111) faces gradually grow from a flocked nucleus into sharp nanothorn structures (see graphic). Large-scale Ag (111) faces are obtained because of its low surface energy.

Palladium Chemistry

*R. Gerber, T. Fox, C. M. Frech** .... 6771 – 6775

P Csp^3 P and P Csp^2 P Palladium(II) Hydride Pincer Complexes: Small Structural Difference—Large Effect on Reactivity

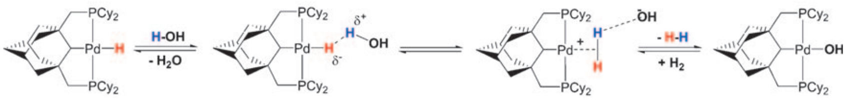

Little and large! The aliphatic palladium(II) pincer hydride complex undergoes smooth dihydrogen evolution and formation of the stable palladium(II) hydroxide complex when an excess of water is added to a solution of the complex in THF. This reactivity is strikingly different when compared to its aromatic analogue and can be attributed to the stronger *trans* influence of the aliphatic pincer unit. The reaction is reversible and fast hydrogenolysis is observed (see scheme).

FULL PAPERS

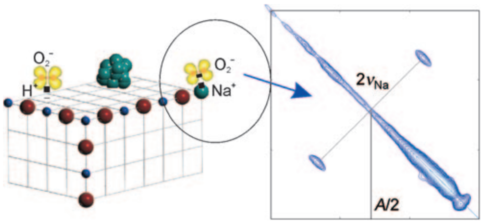

Superoxide to the rescue! Na atoms deposited on polycrystalline MgO samples are brought into contact with O_2 molecules, which are then reduced to superoxide species that are anchored at different surface sites. HYSCORE in combination with DFT calculations enables the local environment of the different superoxide species to be revealed (see figure).

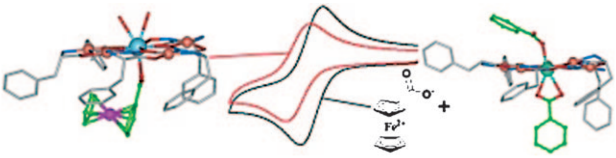

A novel competitive binding assay was used to voltammetrically monitor the binding of a redox-inactive guest to a redox-inactive metallacrown host (see scheme). Binding constants were determined based on the shift in the potential of a ferrocene carboxylate redox probe in the presence of the host and guest.

Two series of novel platinum(II) 2,6-bis(1-alkylpyrazol-3-yl)pyridyl (N5C*n*) complexes, [Pt(N5C*n*)Cl][X] and [Pt(N5C*n*)(C≡CR)][X] (X = trifluoromethanesulfonate (OTf) or PF_6; R = C_6H_5, C_6H_4-*p*-CF_3, and C_6H_4-*p*-N(C_6H_5)$_2$), have been successfully synthesized and characterized. Two amphiphilic platinum(II) 2,6-bis(1-tetradecylpyrazol-3-yl)pyridyl (N5C14) complexes were found to form stable and reproducible Langmuir–Blodgett (LB) films at the air–water interface (see graphic).

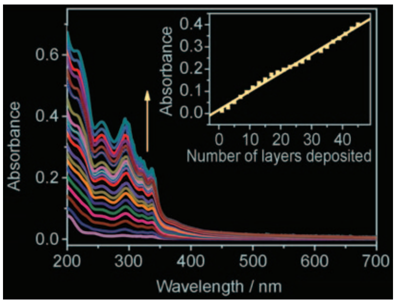

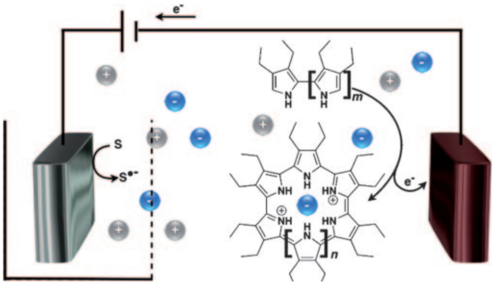

Anion templates: Appropriately sized anions have been shown to act as templates that favor the electrochemical oxidative conversion of pyrrole-containing building blocks into cyclo[*n*]pyrrole (see graphic; *m* = 0 or 1, *n* = 2 or 3; S = solvent).

Catalysis

*J. H. Dam, G. Osztrovszky, L. U. Nordstrøm, R. Madsen** .... 6820 – 6827

Amide Synthesis from Alcohols and Amines Catalyzed by Ruthenium N-Heterocyclic Carbene Complexes

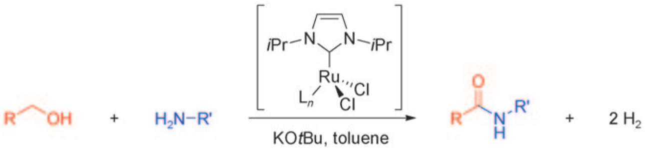

Amides from alcohols: Ruthenium N-heterocyclic carbene complexes catalyze the direct formation of amides from alcohols and amines in the absence of any stoichiometric additives or oxidants (see scheme). Three different catalyst systems are presented that all employ 1,3-diisopropylimidazol-2-ylidene as the carbene ligand.

Cyclic Carbonates

W. Clegg, R. W. Harrington, M. North, R. Pasquale* .... 6828 – 6843

Cyclic Carbonate Synthesis Catalysed by Bimetallic Aluminium–Salen Complexes

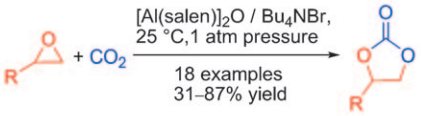

Waste not want not: A combination of bimetallic aluminium–salen complexes and tetrabutylammonium bromide catalyses the formation of cyclic carbonates under exceptionally mild reaction conditions (see scheme). The aluminium catalysts can be reused over 60 times and in situ FTIR has allowed a full analysis of the reaction kinetics.

Coordination Chemistry

*S. Metz, B. Theis, C. Burschka, R. Tacke** .... 6844 – 6856

Neutral Pentacoordinate Halogeno- and Pseudohalogenosilicon(IV) Complexes with an SiSONCX Skeleton (X = F, Cl, Br, I, N, C): Synthesis and Structural Characterization in the Solid State and in Solution

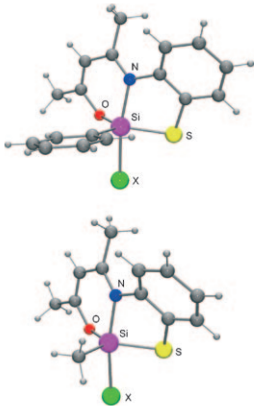

Silicon complexes: A series of neutral pentacoordinate silicon(IV) complexes with Si–X bonds (e.g., X = F, Cl, Br, I) was synthesized (see figure for examples) and structurally characterized both in the solid state and in solution. Solution-state NMR studies revealed the existence of an equilibrium between these compounds and isomeric tetracoordinate species, with the following trend for favoring the pentacoordinate species: I ≈ Br > Cl > F.

Alcohol Oxidation

*C. Berini, O. H. Winkelmann, J. Otten, D. A. Vicic, O. Navarro** . . . 6857 – 6860

Rapid and Selective Catalytic Oxidation of Secondary Alcohols at Room Temperature by Using (N-Heterocyclic Carbene)–Ni^0 Systems

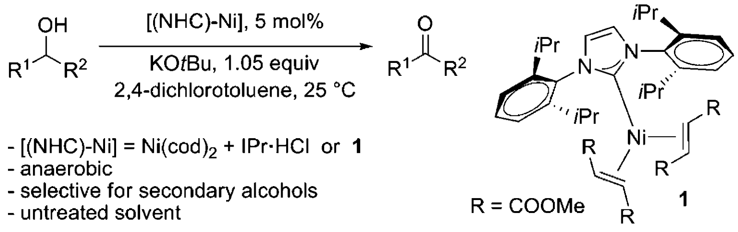

Well defined: The development of both in situ and well-defined [(NHC)–Ni] systems for the selective, catalytic oxidation of secondary alcohols is presented (see scheme; IPr·HCl = 1,3-bis(2,6-diisopropylphenyl)imidazolium chloride). The use of untreated 2,4-dichlorotoluene as both solvent and oxidant allows for high yields even at room temperature.

The stability of boryl radicals complexed with Lewis bases (see scheme) has been studied at the G3(MP2)-RAD level. The analysis of charge- and spin-density distributions shows that spin delocalization in the boryl radical complexes constitutes one of the mechanisms of radical stabilization.

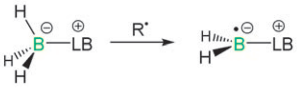

Radicals

All mixed up! A new series of mixed thiophene–pyrrole functionalized oligomers has been prepared and the electronic benefits arising from the combination of these two heterocycles investigated. An analysis of their spectroscopic, photophysical, electrochemical, solid-state, and vibrational properties (see figure) has been performed in combination with quantum-chemical calculations.

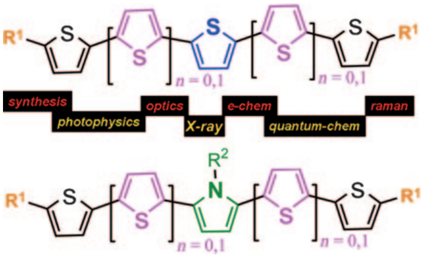

Organic Semiconductors

DNA modification: A simple, modular, regioselective, and efficient Cu-free click reaction of nitrile oxides with styrene-modified DNA (9 and 300 bp) is presented (see scheme). This click reaction on highly modified PCR fragments results in the efficient functionalization of hundreds of styrenes on large DNA fragments. Sequential labeling of PCR products by Cu-free and Cu-catalyzed click reactions was also achieved.

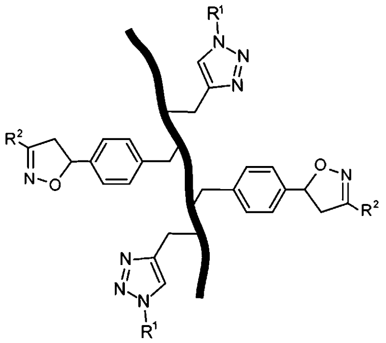

DNA Labeling

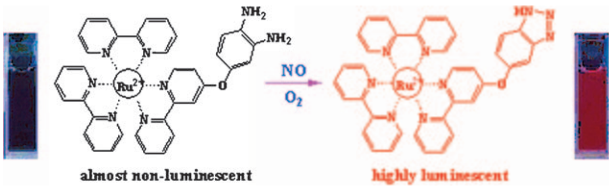

NO problem solved: A unique ruthenium(II) complex, bis(2,2′-bipyridine)(4-(3,4-diaminophenoxy)-2,2′-bipyridine)ruthenium(II) hexafluorophosphate, has been designed and synthesized as a highly sensitive and selective luminescent probe for NO (see picture). The application of the probe for imaging of NO production in living cells was investigated. The results demonstrated the efficacy and advantages of the new probe for the in vivo detection of NO.

Luminescent Imaging Agents

Homogeneous Catalysis

*C. Ohde, C. Limberg** 6892–6899

From Surface-Inspired Oxovanadium Silsesquioxane Models to Active Catalysts for the Oxidation of Alcohols with O_2—The Cinnamic Acid/Metavanadate System

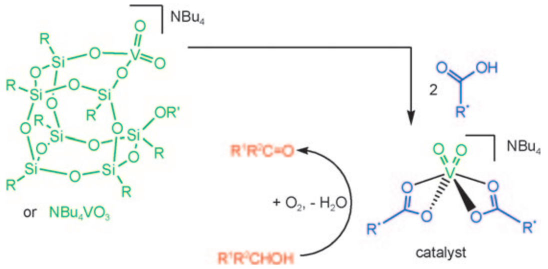

Serendipity works! An investigation concerning the reactivity of silsesquioxane dioxovanadates led to the discovery of an efficient, easily accessible catalyst for the oxidative dehydrogenation of alcohols that utilizes O_2 and functions via peroxo intermediates.

Gene Expression

*P. Wang, C.-H. Leung, D.-L. Ma, S.-C. Yan, C.-M. Che** 6900–6911

Structure-Based Design of Platinum(II) Complexes as c-*myc* Oncogene Down-Regulators and Luminescent Probes for G-Quadruplex DNA

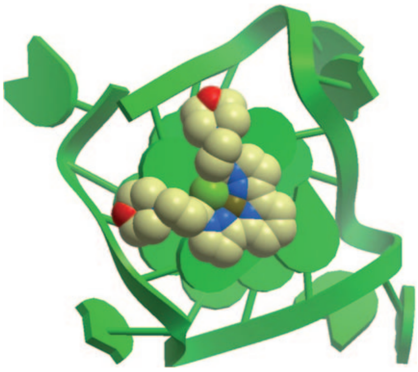

Right on target: By using a computer-aided, structure-based approach, we designed Pt^{II} complexes containing extended planar π-conjugated tridentate ligands with linked amine side-chains that effectively stabilize the c-*myc* G-quadruplex (see figure) and down-regulate c-*myc* transcription. The complexes exhibit strong emission in the presence of G-quadruplex DNA but not duplex DNA and thus have potential uses as luminescent probes.

Supramolecular Chemistry

M. A. Kostiainen, J. Kotimaa, M.-L. Laukkanen, G. M. Pavan* 6912–6918

Optically Degradable Dendrons for Temporary Adhesion of Proteins to DNA

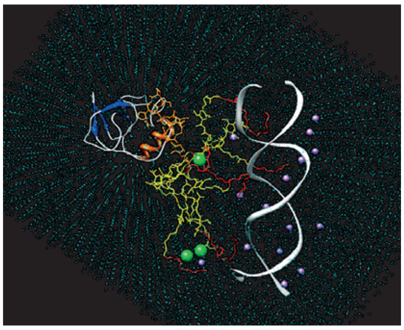

Glue for proteins and DNA: Experimental studies and molecular dynamics modeling demonstrates that multivalent dendrons can be utilized to temporarily glue proteins and DNA together with high affinity (see figure). UV exposure can degrade the photolabile surface of the dendron, which results in loss of the multivalent binding interactions and release of the DNA and protein.

NMR Spectroscopy

V. de la Fuente, M. Waugh, G. R. Eastham, J. A. Iggo,* S. Castillón, C. Claver** 6919–6932

Phosphine Ligands in the Palladium-Catalysed Methoxycarbonylation of Ethene: Insights into the Catalytic Cycle through an HP NMR Spectroscopic Study

Palladium complexes containing bulky bidentate phosphines with a cycloalkyl backbone are very active systems in the methoxycarbonylation of ethene. The basicity of the ligands plays an important role in the catalytic process because it determines the pK_a of the acid that has to be used in the catalytic reaction. An NMR spectroscopy mechanistic study has established the catalytic cycle and has demonstrated that, in this case, the resting state is the $[Pd(O_2CCF_3)(P\text{-}P)]^+$ precursor and not the [Pd]–H (see scheme).

Natural Products

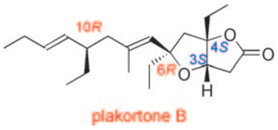

Configuration confirmed: All four possible absolute configurations of plakortone B were synthesized and one of these molecules was found to be identical to natural plakortone B on the basis of ^{1}H and ^{13}C NMR spectra and specific rotation comparisons. Thus, the absolute configuration of natural plakortone B was determined to be (3*S*,4*S*,6*R*,10*R*).

Alkanes

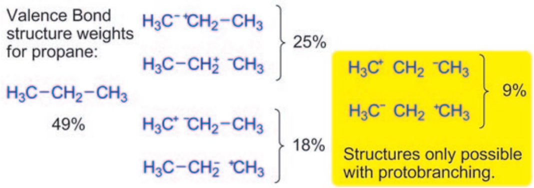

Protobranching—paradigm-shifting or folly? The protobranching and geminal steric hypotheses concerning the greater stability of branched alkanes were investigated. Our results support a stabilizing interaction as being responsible for the phenomenon that also manifests itself in linear alkanes as small as propane. We identify geminal σ→σ* excitations as responsible for this stability as represented by the highlighted structures (see scheme).

Rotaxanes

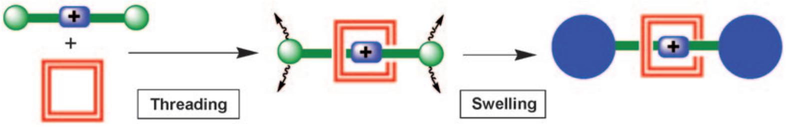

Through the eye of a needle: A "threading-followed-by-swelling" protocol has been developed to synthesize symmetrical and asymmetrical [2]rotaxanes, featuring one of three different types of interlocked macrocycle, in an efficient and atom-economical manner (see figure).

Photochemistry

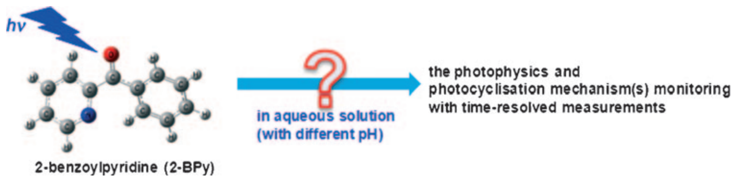

Photocyclisation mechanisms: After laser photolysis, the ultrafast photophysics and photocyclisation reactions of 2-benzoylpyridine (2-BPy) were monitored by femtosecond transient absorption (fs-TA) and nanosecond time-resolved resonance Raman spectroscopy (see figure). These results combined with density functional theory calculations have allowed a detailed analysis of the photocyclisation mechanism(s) in aqueous solvent at different pH values.

Self-Assembly

I. Ling, Y. Alias, A. N. Sobolev, L. T. Byrne, C. L. Raston** 6973 – 6982

Selective Binding of Imidazolium Cations in Building Multi-Component Layers

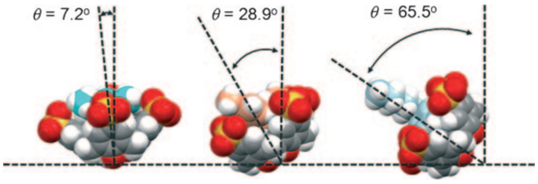

Flexible interplay: Selective binding of different imidazolium cations (C_n-mim) into the cavities of calixarenes affords a multi-layered material with an inherently flexible interplay of the components. Incorporation of ethyl, *n*-butyl or *n*-hexyl imidazolium cations into the multi-component layers of *p*-sulfonated calix[4]arene results in tilting of the plane of the bowl-shaped calixarene relative to the plane of the multi-layer (see figure).

Enzyme Inhibitors

*D. Pearson, A. D. Abell** . . . 6983 – 6992

Structural Optimization of Photoswitch Ligands for Surface Attachment of α-Chymotrypsin and Regulation of Its Surface Binding

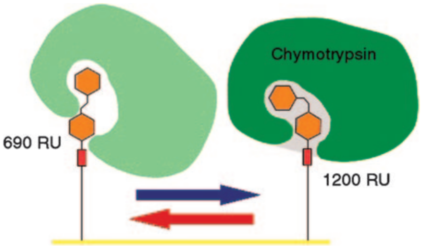

Optimizing photoswitches: In the development of a photoswitch surface, a series of azobenzene-containing trifluoromethyl ketones and α-keto esters with surface attachment groups were synthesized as photoswitch inhibitors of α-chymotrypsin (see figure). The best photoswitch shows a reversible change in IC_{50} of >5.3 times on photoisomerization. A selected inhibitor was used in the development of a photoswitch surface.

Heterogeneous Catalysis

A. Grünberg, X. Yeping, H. Breitzke, G. Buntkowsky** . . . . 6993 – 6998

Solid-State NMR Characterization of Wilkinson's Catalyst Immobilized in Mesoporous SBA-3 Silica

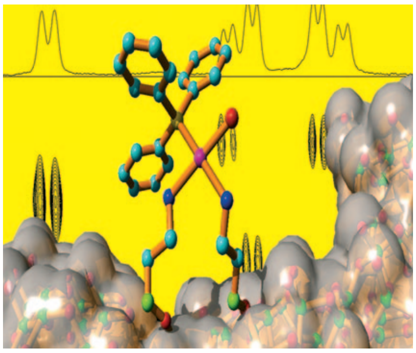

It's magic! By employing a combination of 1D and 2D solid-state NMR techniques, the immobilization of Wilkinson's catalyst $[RhCl(PPh_3)_3]$ on the inner surfaces of mesoporous SBA-3 is shown and the exact mode of binding is revealed by analyzing the ^{31}P–^{31}P spin–spin couplings in the solid state by 2D *J*-resolved magic-angle-spinning NMR spectroscopy.

Transition-Metal Complexes

H. Zhang, R. Lin, G. Hong, T. Wang, T. B. Wen, H. Xia** . . . . 6999 – 7007

Nucleophilic Aromatic Addition Reactions of the Metallabenzenes and Metallapyridinium: Attacking Aromatic Metallacycles with Bis(diphenylphosphino)methane to Form Metallacyclohexadienes and Cyclic η²-Allene-Coordinated Complexes

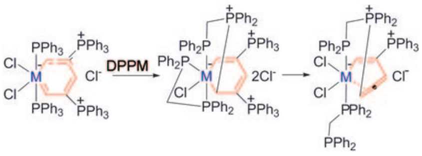

Complex chemistry: The nucleophilic aromatic addition reactions of the phosphonium-substituted metallabenzenes and metallapyridinium with bidentate bis(diphenylphosphino)methane (DPPM) were investigated (see scheme) and provide a simple and efficient method for the synthesis of allene-coordinated metallacycles from the metallaaromatics.

Oxidation

Go detox! The antioxidant action of model polyphenols is examined by ^{1}H CIDNP experiments during the reaction with the excited triplet state of ITX (see scheme for examples). Hydrogen abstraction from model polyphenols is found to be in accord with the bond dissociation energies (BDEs) of A- and B-ring phenolic hydrogen atoms. Chemically induced dynamic nuclear polarization (CIDNP) experiments in real beverages (green tea and red wine) show comparable antioxidant chemistry.

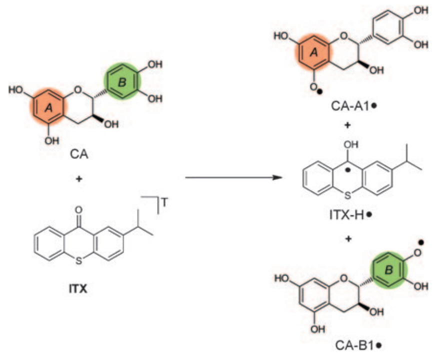

Glycocalix Mimetic

Glyco-SAM formation: The formation of glycol-self-assembled monolayers (glyco-SAMs) on gold surfaces (see figure; EG = ethylene glycol) allows the glycocalyx to be mimicked and has been studied by surface plasmon resonance, a technique that plays a key role in investigating carbohydrate recognition events. In the novel approach reported herein, the anchored mono- and disaccharides are maintained in the closed-ring pyranoside form required for biological recognition.

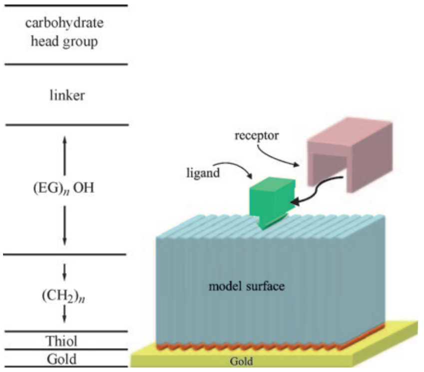

Asymmetric Organocatalysis

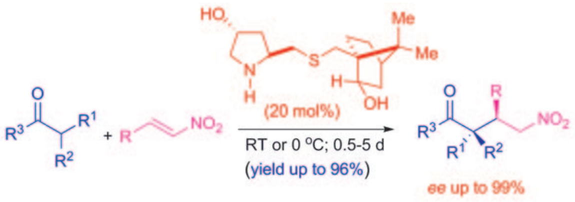

Bi-functional catalysts: Practical and convenient synthetic routes have been developed for the synthesis of pyrrolidinyl–camphor derivatives. These novel compounds were screened as catalysts for the direct Michael addition of symmetrical α,α-disubstituted aldehydes to β-nitroalkenes. The scope of the catalytic system was expanded to encompass the use of various aldehydes and ketones as the donor source (see scheme).

---

* Author to whom correspondence should be addressed

💻 Supporting information on the WWW (see article for access details).

VIP Full Papers labeled with this symbol have been judged by two referees as being “very important papers”.

🎥 A video clip is available as Supporting Information on the WWW (see article for access details).

SERVICE

CHEMISTRY
A EUROPEAN JOURNAL

CORRIGENDUM

*J. Hioe, A. Karton, J. M. L. Martin, H. Zipse** 6861–6865

Borane–Lewis Base Complexes as Homolytic Hydrogen Atom Donors

Chem. Eur. J., **2010**, *16*

DOI: 10.1002/chem.200903395

In Figure 1 of the Full Paper by H. Zipse et al., the structure of compound **22** was found to have been drawn incorrectly. The corrected structure is shown in the new version of Figure 1 given below. Additionally, the data for compounds **18** and **22** were interchanged in Table 2; the values are shown in the correct order here and the compounds have been reordered in Figure 1 as a consequence. Lastly, a recalculation of the data in Tables 1 and 2 indicated a round-off error of 0.3 kJ mol^{-1} for compound **14** in Table 2. The changes do not affect the conclusions of the manuscript, and the authors apologize for any inconvenience caused by these errors.

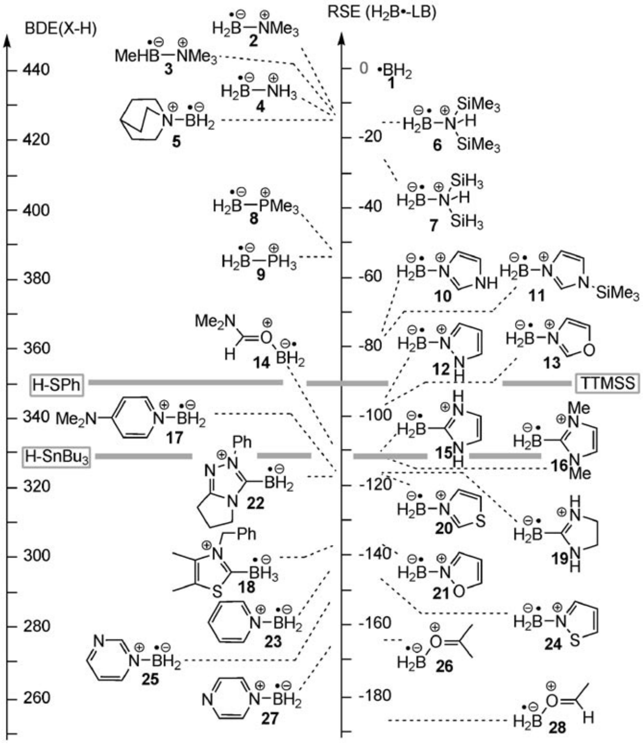

Figure 1. Radical stabilization energies (RSE, in kJ mol^{-1}) for a variety of boryl radicals as obtained at G3(MP2)-RAD level of theory together with the BDE(B−H) values of the corresponding boranes.

Table 2. Radical stabilization energies (RSE) for a variety of boryl radicals together with the BDE(B−H) values of the corresponding boranes, the complexation energies of borane–Lewis base complexes (E_c(H$_3$BLB)), and complexation energies of boryl radical–Lewis base complexes (E_c(H$_2$B$^•$LB)). All energies have been obtained at G3(MP2)-RAD level and are given in kJ mol^{-1}.

System	RSE(H$_2$B$^•$–LB)	BDE(H–BH$_2$–LB)	E_c(H$_3$BLB)	E_c(H$_2$B$^•$LB)
1	0.0	441.1	–	–
2	−12.6	428.7	−158.3	−170.9
3	−12.8	428.3	−280.8	−139.7
4	−13.7	427.4	−114.1	−127.8
5	−14.0	427.1	−170.6	−184.6
6	−16.7	424.4	−99.9	−116.7
7	−24.6	416.5	−158.3	−113.8
8	−52.1	389.0	−159.9	−212.0
9	−54.3	386.8	−91.4	−145.6
10	−77.3	363.8	−136.7	−213.9
11	−79.4	361.7	−142.8	−222.2
12	−95.2	345.9	−129.0	−224.2
13	−97.9	343.2	−119.7	−217.6
14	−108.9	332.2	−84.1	−193.0
15	−110.7	330.4	−220.6	−331.3
16	−112.5	328.6	−228.0	−340.5
17	−116.3	324.8	−147.5	−263.8
18	−138.7	302.4	−216.0	−354.7
19	−116.9	324.2	−228.1	−345.0
20	−117.7	323.4	−124.4	−242.0
21	−137.2	303.9	−107.3	−244.5
22	−116.6	324.5	−211.1	−327.7
23	−144.3	296.8	−132.0	−276.3
24	−146.6	294.5	−109.2	−255.8
25	−152.5	288.6	−126.1	−278.6
26	−163.6	277.5	−73.6	−237.2
27	−165.8	275.3	−126.5	−292.2
28	−184.0	257.1	−66.1	−250.1